

Size effects in optical second-harmonic generation by metallic nanocrystals and semiconductor quantum dots: The role of quantum chaotic dynamics

O. A. Aktsipetrov, P. V. Elyutin, A. A. Nikulin, and E. A. Ostrovskaya

Physics Department, Moscow State University, Moscow 119899, Russia

(Received 1 July 1993; revised manuscript received 8 June 1994)

Second-harmonic generation in small metallic nanocrystals and semiconductor quantum dots is studied both experimentally and theoretically. The enhancement of the nonlinear optical response with the decrease of the particle radius from 100 to about 10 Å has been experimentally observed. The theoretical description based on the model of chaotic motion of noninteracting electrons in the particles agrees satisfactorily with the experimental data.

I. INTRODUCTION

The unique physical properties of metallic nanocrystals (MN) and semiconductor quantum dots (QD) have been attracting researchers attention for the past few years. The primary concern is with the experimental observation and proper understanding of various quantum size effects in these quasi-zero-dimensional systems¹ which can be used as nanometer-size structural components in composite materials and ultrafast optoelectronic devices (such as switches, memory cells, etc.).

The spatial confinement of electrons in QD and MN strongly affects both the linear and nonlinear optical properties of the systems. The enhancement of the optical nonlinearity of QD (in comparison with that of the bulk semiconductor) is predicted in Ref. 2 for the case when the size quantization of the exciton motion is taken into account. For semiconductor microcrystallites embedded in glass matrices various nonlinear optical effects described by third-order susceptibility have been studied experimentally: degenerate four-wave mixing,³ nonlinear absorption,⁴ and encoded second-harmonic generation.⁵ It should be noted that up to the present time the third-order (cubic) optical nonlinearity of QD has been studied to a much greater extent than the second-order (quadratic) one. Experimentalists preferred the cubic effects because the quadratic effects, such as reflected second-harmonic (SH) generation, appeared to be negligibly small in macroscopic arrays of QD and MN considered (at the macroscopic level) as centrosymmetric media. The measurements of size dependence of reflected SH generation in metal and semiconductor nanostructures were reported in Ref. 6.

The theoretical study of the nonlinear optical response of small particles demands the departure from the standard solid-state theory of the bulk materials. Since the noticeable fraction of atoms in a small particle belongs to its surface, the influence of the particle shape becomes very important. In many theoretical models for optical response of small particles (MN and QD) the particle shape is supposed to be centrosymmetric, most often spherical.⁷ However, in a more realistic approach to studying quadratic optical effects in nanometer-size parti-

cles the fluctuations of the particle shape should be taken into account. These fluctuations (being the generic feature of mesoscopic systems) cannot be ignored for at least two reasons. First, the quadratic susceptibility of a centrosymmetric system is equal to zero in the dipole approximation. Therefore, one may expect that even small shape distortions breaking the inversion symmetry of the particles lead to a noticeable enhancement of second-order optical response due to the appearance of nonzero dipole quadratic susceptibility. Second, the deviations from the exact symmetry may demolish the integrability of the electron motion. Then the electron in a small particle should be described by a model of a quantum chaotic system. Its energy spectrum, wave functions of stationary states, and matrix elements of dynamical variables become random quantities that should be described statistically.^{8,9} It is worth noting that in such a case one has to deal with two basically distinct sources of irregularity of physical quantities. The first one is the mesoscopic nature of the system revealing itself in fluctuations of the particle shape and other parameters characterizing the system. The second source is the stochasticity of the electron dynamics that occurs for any given particle shape that demolishes the integrability of the electron motion.

This approach has its history. The model of the completely random Hamiltonian that belongs to the Gaussian ensemble was applied to the electrons in small metallic particles by Gor'kov and Eliashberg.¹⁰ Much later, along with the development of the classical theory of the chaotic dynamics, the applicability of such a model has been connected to the measure of the stochastic component of the energy surface of the classical counterpart of the system.^{11,12} Although this connection has been derived from the analysis of the two-dimensional systems (billiards and nonlinear oscillators), its relevance to the three-dimensional case is universally accepted. However, to our knowledge, no systematic study of the nonlinear optical properties of MN and QD in terms of quantum chaotic dynamics has been carried out previously and no proper model for the calculation of the quadratic susceptibility has been established.

In this paper the dependence of quadratic optical response of MN and QD on the mean particle size is in-

vestigated both experimentally and theoretically. In our experimental studies the reflected SH generation technique is used. In the theoretical interpretation of the observed size effects special emphasis is put on the role of stochasticity of the electron motion. In the model proposed for the calculation of the response of small particles we use two basic concepts. First, we consider the energy intervals and the matrix elements of the model to be random quantities with the statistical properties taken from the theory of strongly chaotic quantum systems. Second, to evaluate the coarse-grained behavior of these variables smoothed over energy intervals that contain many energy levels of the system, we use the correspondence principle. For example, we replace the average square of the matrix element of a dynamic variable by the properly scaled spectral density of its classical analog.¹³ The size dependence of the quadratic susceptibility in the chaotic model is compared with those obtained in the alternative approach based on the regular model.

II. EXPERIMENT

A. Metallic nanocrystallites

The size dependence of the surface-enhanced second-harmonic generation was studied in the silver island films (IF) with the ultrasmall particles. The samples of IF were prepared by evaporation of all components in an ultrahigh vacuum chamber with residual pressure about 10^{-9} Torr. The surface of the sodium chloride monocrystals covered with a thin film of silicon monoxide (SiO_x) was used as a substrate for IF. While in the vacuum chamber before the deposition the sodium chloride crystals were heated to 700 K to clear their surface. The silicon monoxide layers 50 nm thick were deposited at a rate of 0.2 nm s^{-1} . Silver was evaporated on the SiO_x layer by a calibrated source with the same rate of 0.2 nm s^{-1} . After the silver nanocrystallite deposition the island films were again covered with an amorphous SiO_x layer 50 nm thick to protect the metal nanocrystallites from environment.

After the complete evaporating procedure the initial substrates were cleaved into samples for nonlinear optical experiments and transmitting electron microscopy. The typical structure of silver island films is shown in Fig. 1. Using a JEM 100 C transmitting electron microscope we determined the following parameters of the films: the average particle radius \bar{R} ranged from 1 to 10 nm, mass thickness d_m ranged from 0.1 to 3.4 nm, and filling factor q ranged from 0.07 to 0.4. The characteristic particle radius was found by taking an average over several hundred islands. The histograms of the corresponding distribution functions are presented in Fig. 2.

The island films were irradiated by a Q -switched YAG: Nd^{3+} (yttrium aluminum garnet) laser (pulse duration 15 ns, repetition rate 12.5 Hz). The incident TEM_{00} radiation with wavelength $\lambda = 1064 \text{ nm}$ was p polarized. The SH intensity measurements were carried out at the value of the pump intensity $I_\omega \sim 0.5 \text{ MW/cm}^2$. No sample damage has been observed for this intensity. The SH radiation was marked out by a double monochromator,

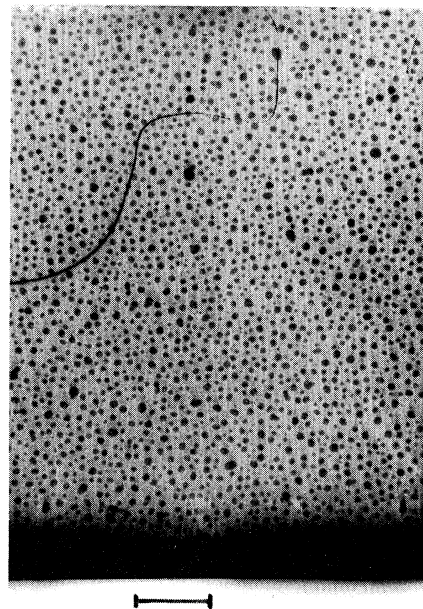


FIG. 1. Typical structure of a silver island film as observed in transmitting electron microscope. The bar is 20 nm long.

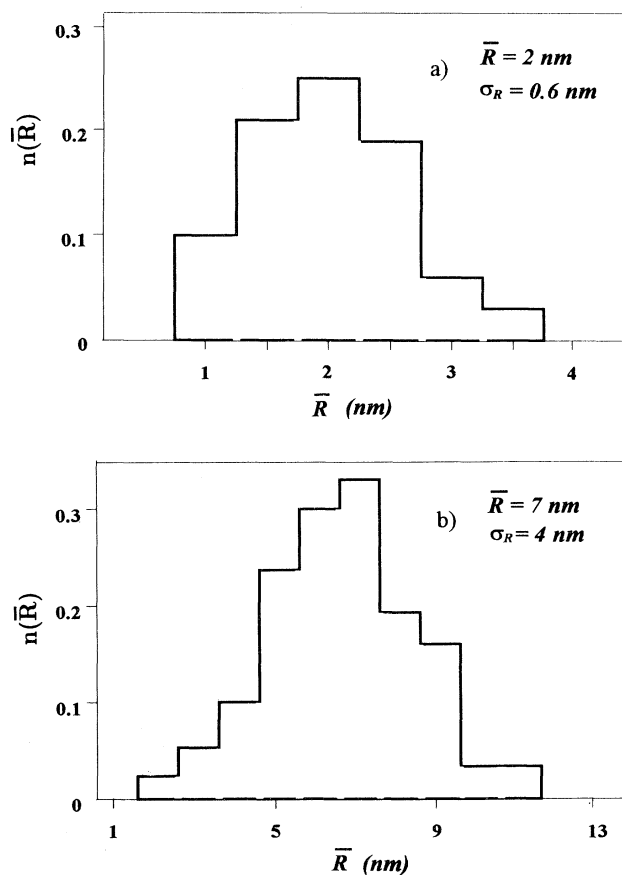


FIG. 2. Histograms $n(\bar{R})$ of the size distribution functions (relative number of particles with the average radius \bar{R}) for two samples (a) and (b) of silver island films. σ_R is the standard deviation of the particle radius.

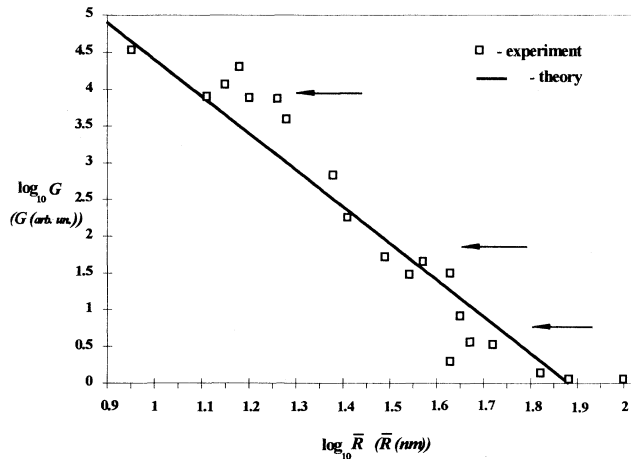


FIG. 3. The SH enhancement factor G as a function of the average radius \bar{R} of silver particles (\bar{R} is measured in nanometers). The arrows indicate the peculiarities of the experimental size dependence.

and its intensity $I_{2\omega}$ was detected by photomultiplier and conventional gated electronics. The calibration of the electronic detection system was performed with the help of reflected SH generation at the surface of the bulk silver sample. For this material a value of $I_{2\omega}/I_{\omega}^2 = 1.4 \times 10^{-27}$ cgs units is well known.¹⁴

The film samples differed in the average island radius \bar{R} as well as in the surface concentration of islands $n^{(Ag)}$, so that the filling factor $q^{(Ag)} = \pi n^{(Ag)} \bar{R}^2$ varied from sample to sample. It should be emphasized in this connection that the measured value of the SH intensity $I_{2\omega}$ cannot characterize explicitly the size effect in the quadratic optical response of the islands since in our experiments $I_{2\omega}$ varied as a function of two arguments, \bar{R} and $q^{(Ag)}$ (or \bar{R} and $n^{(Ag)}$). For that reason, in order to select the pure size effect, the measured values of the SH signal were normalized in accordance with the procedure described in Sec. II C. The corresponding dependence is shown in Fig. 3.

B. Semiconductor quantum dots

In the present experiments the reflected SH was generated upon the reflection of a YAG:Nd³⁺ laser beam with wavelength of 1064 nm from the surface of a composite material consisting of CdSe nanocrystals embedded in a glass matrix. Other details of the SH measurements are described in Sec. II A.

The investigated sample of semiconductor-doped glass was prepared by a method of secondary heat treatment.¹⁶ The cadmium selenide concentration was about 0.5% of volume fraction and uniform over the bulk of the glass bar. The average size of the nanocrystals varied from 50 to 5 nm for various parts of the glass bar because of the special secondary heat procedure. The monotonous character of the average size variation along the sample was monitored by the spectral shift of the absorption band

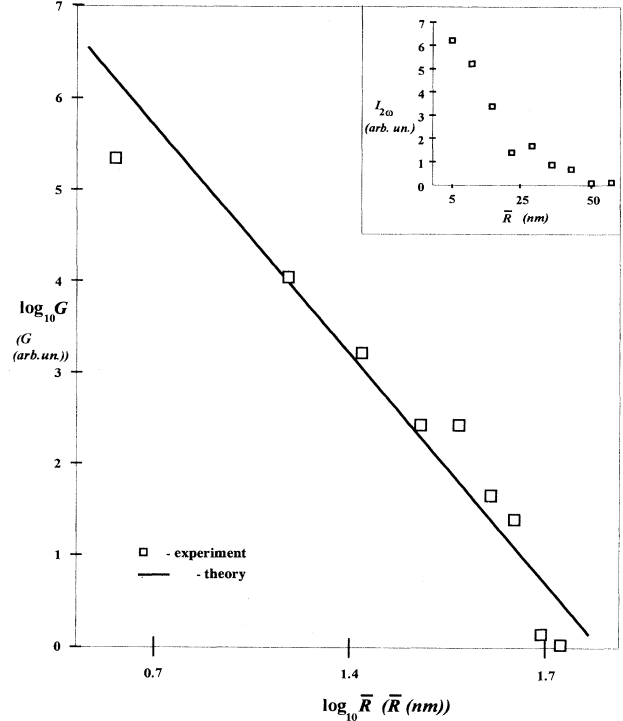


FIG. 4. The SH enhancement factor G as a function of the average radius \bar{R} of CdSe crystallites (\bar{R} is measured in nanometers). The inset shows the SH intensity $I_{2\omega}$ (in arbitrary units) measured as a function of \bar{R} .

edge.

Thus for the sample studied the filling factor $q^{(CdSe)} = (4\pi/3)n^{(CdSe)}\bar{R}^3$ (where $n^{(CdSe)}$ is the volume concentration of CdSe crystallites) was constant due to the preparation technique. This allowed us, in contrast with the case of silver island films, to treat the measured SH intensity as a function of a single variable \bar{R} (see the inset in Fig. 4). The experimental data, normalized as described in Sec. II C, are shown in the main panel of Fig. 4.

C. Handling of the experimental data

In our experiments the SH radiation was generated upon reflection of laser light from a macroscopic disordered two- (silver island film) or three-dimensional (CdSe crystallites in a glass matrix) array of particles. To select the pure size effect in the quadratic optical response of the particles one needs to obtain an expression relating the measured value of the SH intensity with the effective second-order susceptibility of a single particle $\chi_2 \equiv \alpha_2/V$ (where α_2 and V are the quadratic polarization and volume of the particle, respectively). The particles may be treated as pointlike dipoles oscillating at SH frequency since the parameters of the systems under study satisfy the inequalities

$$\bar{R} \ll \bar{l} \ll \lambda_{\omega}, \quad (1)$$

where \bar{R} is the average particle size, \bar{l} the average dis-

tance between neighboring particles, and λ_ω the pump wavelength. For silver islands $\bar{I}^{(\text{Ag})} \sim n^{(\text{Ag})-1/2}$, for CdSe crystallites $\bar{I}^{(\text{CdSe})} \sim n^{(\text{CdSe})-1/3}$, where $n^{(\text{Ag})}$ ($n^{(\text{CdSe})}$) is the surface (volume) concentration of the particles. The detected SH radiation from both metal and semiconductor particles was diffuse and depolarized, thus substantiating the fluctuational nature of the nonlinear optical sources:

$$|\overline{\chi_2}|^2 \gg |\chi_2|^2, \quad (2)$$

where the overbar denotes averaging over the ensemble of particles. Taking into account the inequalities (1) and (2) one can write for the measured intensity of the diffuse SH component generated by a disordered array of particles the relation

$$I_{2\omega}^{(\text{exp})} \propto n \bar{V}^2 |L(2\omega, q) L^2(\omega, q)|^2 |\overline{\chi_2(\omega)}|^2 I_\omega^2. \quad (3)$$

Here $n = n^{(\text{Ag})}$, $n^{(\text{CdSe})}$, \bar{V} is the average particle volume, I_ω is the pump intensity, and $L(\omega)$ and $L(2\omega)$ are the local field factors describing average local field corrections due to the linear response of particles at the pump and the second-harmonic frequency, respectively (it is assumed that the fluctuations of the local field factor and the particle volume are negligibly small in contrast to those of the quadratic susceptibility). The local field factor depends on the local environment of particles and, as a result, turns to be a function of the filling factor q ($q = q^{(\text{Ag})}$, $q^{(\text{CdSe})}$).

Thus the dependence $\chi_2(\bar{R})$ is determined by the normalized SH intensity:

$$\begin{aligned} |\chi_2(\bar{R})|^2 &\propto I_{2\omega}^{(\text{norm})}(\bar{R}) \\ &\equiv \frac{I_{2\omega}^{(\text{exp})}(\bar{R})}{I_\omega^2 n \bar{V}^2 |L(2\omega, q^{(\text{Ag})}) L^2(\omega, q)|^2}. \end{aligned} \quad (4)$$

In order to express the denominator in the right-hand side of Eq. (4) as a known function of the measured parameters \bar{R} , q , we have used the following additional approximations.

(i) The particle shape distortions are supposed to be sufficiently small to neglect their influence on $L(2\omega, q)$ and \bar{V} [therefore $\bar{V} = (4\pi/3)\bar{R}^3$]. At the same time these distortions are of key importance for the calculation of $|\chi_2|^2$ —see Sec. III.

(ii) The linear-optical response of the particle is described with the local (bulk) dielectric constant: It is assumed that the size-dependent nonlocal effects are negligible within the available size ranges ($1 \text{ nm} \leq \bar{R}^{(\text{Ag})} \leq 10 \text{ nm}$, $5 \text{ nm} \leq \bar{R}^{(\text{CdSe})} \leq 50 \text{ nm}$).

(iii) The values of $L(\omega, q)$ was calculated using the expression obtained in Ref. 15 within the framework of a simple effective-medium approximation.

Finally, the enhancement factor describing the size dependence of the quadratic optical response was defined as follows:

$$G(\bar{R}) \equiv I_{2\omega}^{(\text{norm})}(\bar{R}) / I_{2\omega}^{(\text{norm})}(\bar{R}_{\text{max}}), \quad (5)$$

where $\bar{R}_{\text{max}}^{(\text{Ag})} \sim 10 \text{ nm}$, $\bar{R}_{\text{max}}^{(\text{CdSe})} \sim 50 \text{ nm}$.

The experimental dependence $G(\bar{R})$ is shown in Fig. 3

for silver islands and in Fig. 4 for CdSe crystallites. One can see that the enhancement of the quadratic response upon decrease in the particle size amounts to 6 orders of magnitude for metal particles and 5 orders of semiconductor ones.

III. THEORY

A. The model

We shall treat a particle as a system of noninteracting electrons confined by the impenetrable boundary surface of nearly spherical form with average radius \bar{R} . Later this surface will be called a (three-dimensional) billiard. The electrons' interaction with the crystal lattice will be taken into account by the dispersion law borrowed from the bulk material.

Since the intraband transitions are taken into account in the metallic particles and interband optical transitions in the semiconductor particles with two different energy bands, the electron mass m should be considered as the effective mass m_{eff} for both types of particles. For the metallic particle m_{eff} is the mass of conduction electron and for every energy band in the semiconductor m_{eff} has a specific value.

Because of the irregularity of the billiard form the classical motion of electrons, elastically reflecting from the boundary, will be considered as completely ergodic on the energy surface. The quantum properties of the electronic states accordingly will be imported from the random matrix theory.

Let E_n be the energy eigenvalue and λ_n the typical length of the space volume available to an electron with energy E_n . The system can be considered quasiclassical if the inequality

$$\xi_n = [\hbar^2 / 2mE_n \lambda_n^2]^{1/2} \ll 1 \quad (6)$$

holds; for the billiards $\lambda_n \approx \bar{R}$.

For metallic particles m can be identified with the electron rest mass m_e , and the value E_n can be estimated by the Fermi energy E_F . For the semiconductor particles one can take the value E_n from the range $0 < E_n \leq 2\hbar\omega - E_g$ where $\hbar\omega$ is the energy of the radiation quantum and E_g is the width of the energy gap.

Inserting numerical values in (6), one can see that our model appears to be always quasiclassical for the metallic case ($\xi_n \approx 10^{-2}$) and can be quasiclassical for the semiconductor case ($10^{-2} < \xi_n < 1$). That justifies the appeal to the correspondence principle in the following.

B. The quadratic susceptibility

By analogy with the linear susceptibility, one can assume that the effective quadratic susceptibility of the electron in the external static potential is the full dipole moment of the particle divided by the volume.

The quantum expression for the typical component $\chi_2 \equiv \chi^{\text{xxx}}(2\omega)$ of the tensor of effective quadratic susceptibility of the electron to the electric field with the frequency ω in the dipole approximation has the form¹⁷

$$\chi_2 = \frac{e^3}{2\hbar^2} \sum_{nmk} \frac{x_{nm} x_{mk} x_{kn}}{(\omega_{mn} - 2\omega - i\delta_{mn})(\omega_{kn} - \omega - i\delta_{kn})}. \quad (7)$$

Here n, m, k are indices of the eigenstates of electrons belonging to the discrete energy spectrum, x_{ij} is the matrix element of the Cartesian coordinate between the states, ω_{ij} is the frequency of the corresponding transition, and δ_{ij} is the relaxation parameter. The summing over all electrons within the particle billiard can be replaced by the summation over the states n of individual electrons in (7). Matrix elements in (7) have properties which are generic for the matrix elements of dynamical variables in the quantum chaotic system.¹³ On the energy scale $[\rho(E_n)]^{-1} \ll \Delta E \ll E_n$, where $\rho(E_n)$ is the averaged density of energy levels, matrix elements behave as statistically independent random variables. The probability distribution of the off-diagonal elements x_{ij} is Gaussian with a zero mean. Therefore, nonlinear susceptibility of the chaotic system χ_2 should be treated as a statistical quantity.

The rigorous statistical analysis of the quadratic susceptibility is beyond the means of existing theory. We shall simplify the problem by the assumption that the fluctuations of the denominator of expression (7) are negligible due to the repulsion of levels in the energy spectrum of the chaotic system.^{8,9} That allows us to consider the level sequence as a nearly equidistant one and the denominator as a regular quantity. We use $E_n \equiv \hbar\omega_n \approx \hbar n\omega_0$ where $\hbar\omega_0$ is the average energy difference between the levels $\hbar\omega_n \approx [\rho(E_n)]^{-1}$. Then we have

$$\chi_2 = \sum_n \frac{A_n}{\Delta_n^{(1)} \Delta_n^{(2)}}, \quad (8)$$

where

$$\begin{aligned} \Delta_n^{(1)} &= (\omega_{mn} - 2\omega - i\delta) \cong (n\omega_0 + \Delta^{(1)} - i\delta), \\ \Delta_n^{(2)} &= (\omega_{kn} - \omega - i\delta) \cong (n\omega_0 + \Delta^{(2)} - i\delta), \end{aligned} \quad (9)$$

and A_n is the following combination of matrix elements:

$$A_n = \sum_{mk} x_{nm} x_{mk} x_{kn}. \quad (10)$$

$$\chi_2^2 \equiv \sigma_\chi \cong \frac{e^3}{2\hbar^2} \left[\sum_{nmk} \frac{\langle |x_{nm}|^2 \rangle \langle |x_{mk}|^2 \rangle \langle |x_{kn}|^2 \rangle}{[(\omega_{mn} - \omega)^2 + \delta^2][(\omega_{kn} - 2\omega)^2 + \delta^2]} \right]^{1/2}. \quad (14)$$

This quantity can be evaluated in the quasiclassical limit from the correspondence rule¹³

$$\langle |x_{ij}|^2 \rangle |_{\hbar \rightarrow 0} \cong \frac{S(\omega_{ij})}{2\pi\rho(E)}, \quad (15)$$

where $S(\omega)$ is the spectral density of the classical coordinate; $\omega_{ij} \equiv |E_i - E_j|/\hbar$; $E \equiv (E_i + E_j)/2$.

Assuming the particle shape to be almost spherical we can use for the spectral density in our model the expression found in the theory of the stochastic motion in the

The differences $\Delta^{(1)}$ and $\Delta^{(2)}$ are proportional to the level-spacing values: $\Delta^{(1),(2)} \approx \omega_0$. Relaxation constants in Eq. (9) are taken to be equal: $\delta_{mn} \approx \delta_{kn} \equiv \delta$. Then only statistical fluctuations of A_n , the numerator of expression (8), should be considered. Statistical properties of x_{ij} imply that $\langle A_n \rangle = 0$. Here and below, the angular brackets denote averaging over the spectral interval ΔE which contains the large number of energy levels.

The quantities observed in the experiment, such as the intensity of the reflected light, are determined by the averaged squared value σ_χ^2 of χ_2 given by Eq. (8). Because of the Gaussian statistics of the matrix elements x_{ij} it can be expressed by two-point correlation function of A_n :

$$\begin{aligned} \sigma_\chi^2 &\equiv \langle |\chi_2|^2 \rangle \cong \sum_n \frac{\langle |A_n|^2 \rangle}{(\Delta_n^{(1)})^2 (\Delta_n^{(2)})^2} \\ &+ \sum_{nj} \frac{\langle |A_n A_{n+j}| \rangle}{(\Delta_n^{(1)} \Delta_{n+j}^{(1)}) (\Delta_n^{(2)} \Delta_{n+j}^{(2)})}. \end{aligned} \quad (11)$$

We can omit the second sum in (11) on the following grounds. The two-point correlator of the matrix elements of the adjacent pairs of levels in the quasiclassical limit can be replaced by the correlator of the Fourier amplitudes of the corresponding classical dynamical variables:

$$\langle x_{n,n} x_{n+j,n'+j} \rangle |_{\hbar \rightarrow 0} \cong \langle x(\omega) x(\omega') \rangle. \quad (12)$$

Since the classical stochastic motion in a billiard is a stationary random process, the Fourier components of the Cartesian coordinate x are δ correlated:¹⁸

$$\langle x(\omega) x(\omega') \rangle \cong S(\omega) \delta(\omega + \omega'), \quad (13)$$

where $S(\omega)$ is the spectral density of the coordinate. Because of that the two-point correlations such as $\langle |A_n A_{n+j}| \rangle$ are negligible and the second sum in (11) effectively vanishes.

Thus we obtain the estimate of the typical nonlinear susceptibility in our model

nearly circular two-dimensional billiards.¹⁹ The approximate expression for $S(\omega)$, which has a typical error of about 10%, in this case has the form

$$S(\omega) \approx S_A(\omega) = 20\bar{R}^2 \left(\frac{\omega}{\Omega} \right)^6 \quad \text{for } \omega > 2\Omega, \quad (16)$$

and $S(\omega) = 0$ for $\omega < 2\Omega$. The characteristic frequency $\Omega = v/2\bar{R}$, where v is the electron velocity.

The density of levels $\rho(E)$ for the metallic particles can

be calculated straightforwardly:

$$\rho_M(E) \cong \frac{V}{8\sqrt{2}\pi^2} \frac{m^{3/2} E^{1/2}}{\hbar^3}, \quad (17)$$

where $V \approx 4\pi\bar{R}^3/3$ is the volume of a billiard. The electron in the semiconductor particle can be described as the effective metallic system by the use of the combined level density:²⁰

$$\rho_c(E) = \frac{2V}{(2\pi\hbar)^3} \int \delta(E_C(\mathbf{p}) - E_V(\mathbf{p}) - 2\hbar\omega) d\mathbf{p}, \quad (18)$$

where $E_C(\mathbf{p})$ and $E_V(\mathbf{p})$ are the dispersion laws for conduction and valence bands, respectively, and the reduced mass of electron

$$m_r = \frac{m_C m_V}{m_C + m_V}, \quad (18')$$

where m_C and m_V are the effective masses for the conduction and valence bands correspondingly.

C. The symmetry violation

In the centrosymmetric system the matrix element of the coordinate x_{ij} between the states $|i\rangle$ and $|j\rangle$ of the same parity is identically zero, according to the parity selection rule. At least one such element enters in every term of the sum (7); that makes the quadratic susceptibility of spherically symmetric particles vanish: $\chi_2 \equiv 0$. The shape of the small particles with a weakly deformed surface remains close to spherical but the central symmetry can be broken. In the asymmetric particles we assume all classical integrals of motion to be completely destroyed, but parity, the specific discrete integral of motion without the classical analog (at least for a given trajectory), will be only weakly perturbed. The parity P_n of the eigenstate by definition is

$$P_n = \int \Psi_n(\mathbf{r}) \Psi_n(-\mathbf{r}) d\mathbf{r}, \quad (19)$$

where $\Psi_n(\mathbf{r})$ is the wave function of the state $|n\rangle$ in the coordinate representation. The origin of the coordinate system in (19) is chosen at the center of the sphere ap-

proximating the particle form.

If the asymmetry of particle is small, we can expect the absolute values of P_n to be close to unity: $|P_n| \approx 1$. The sign of P_n then can serve for the classification of states as "nearly odd" and "nearly even." The matrix element x_{ij} between the states with a "nearly same" parity may differ from zero. We shall make the simplest assumption that the values of such matrix elements can be estimated as

$$x_{ij} \cong \eta \bar{x}, \quad (20)$$

where \bar{x} is the typical matrix element between the states with "nearly opposite" parities that are given by the quasiclassical asymptotic (15) and η is a dimensionless parameter which describes the degree of deviation of the particle form from the central symmetry.

Let the surface of the particle be described by the equation $r = R(\theta, \varphi)$ where θ and φ are the spherical angles. We assume that the shape function $R(\theta, \varphi)$ has random values with the uniform distribution in (θ, φ) . Then the average deviation from the spherical form is

$$\sigma_r^2 = \frac{1}{\bar{R}^2} \overline{[R(\varphi, \theta) - \bar{r}]^2} = \frac{1}{\bar{R}^2} \int [R(\varphi, \theta) - \bar{r}]^2 d\Omega, \quad (21)$$

where $\bar{r} \equiv \bar{R}$, $d\Omega = \sin\theta d\theta d\varphi$. On the ensemble of different realizations of a random shape of the particle the deviation from sphere σ_r^2 produces some distribution. Then we shall define the coefficient of asymmetry as

$$\eta \approx \overline{\sigma_r}; \quad (22)$$

here the overbar denotes the averaging over the ensemble of realizations, as well as in Eq. (2) (Sec. II C). The value of σ_r^2 can be obtained by additional assumptions.

The irregular nearly spherical surface can be conveniently described by the model of randomly modulated sphere²¹

$$R(\varphi, \theta) = \bar{R} [1 + \varepsilon F(\varphi, \theta)], \quad (23)$$

where $\varepsilon \ll 1$ is the modulation parameter and $F(\varphi, \theta)$ is a random function; its properties are described below.

(i) The function $F(\varphi, \theta)$ can be expanded in a series in spherical harmonics $Y_{lm}(\theta, \varphi)$; only a finite number of terms contribute to this expansion:

$$F(\varphi, \theta) = \sum_{l=N_L}^{N_R} \left\{ \frac{1}{2} A_{l0} P_l(X) + \sum_{m=1}^l (A_{ml} \cos m\varphi + B_{ml} \sin m\varphi) P_l^m(X) \right\}, \quad (24)$$

$$A_{ml} = C_{ml} \alpha_m, \quad B_{ml} = C_{ml} \beta_m, \quad C_{ml} = \left[\frac{2l+1}{2\pi} \frac{(l-m)!}{(l+m)!} \right]^{1/2} X = \cos\theta,$$

where $P_l^m(X)$ is the Legendre associated function.

(ii) The function $F(\varphi, \theta)$ is a random one: the coefficients α_n and β_n are random numbers that take values 1, 0, and -1 with equal probabilities.

(iii) The objects of the study are fine particles of the crystalline materials. So the lattice constant a_0 can serve as the elementary "step" of deformation (or the minimum of modulation amplitude). Then the number of effective

harmonics l may be readily defined as the ratio of length of the arch deformed on the surface to the modulation amplitude:

$$l \approx \bar{R} / za_0, \quad (25)$$

where z is an integer number, and

$$N_L \leq l \leq N_R, \quad (25')$$

$$\max N_R \equiv N_{\max} \approx \bar{R}/a_0, \quad \min N_L \equiv N_{\min} \approx 1.$$

The form parameter, which defines the amplitude of surface modulation by the full number of harmonics $N = (N_R - N_L + 1)^2$, is approximately

$$\varepsilon \sqrt{N} \approx a_0 / \bar{R}. \quad (26)$$

After the definition of $R(\theta, \varphi)$ the degree of asymmetry η can be treated as the degree of modulation characterized by the average deviation from the spherical form. The calculation of σ_r^2 by the formula (21) with the additional averaging over the ensemble of different modulations leads to the expression for the coefficient of asymmetry:

$$\eta \approx \bar{\sigma}_r \approx \varepsilon \sqrt{N} \frac{[(N_R + 1)^2 - (N_L + 1)^2]^{1/2}}{(N_R - N_L + 1)^2}. \quad (27)$$

Thus the coefficient η depends upon two characteristics of particle form: the modulation parameter ε and the full number of harmonics N . Since these parameters are connected to the particle size by Eqs. (25') and (26), the coefficient of asymmetry yields an additional size dependence in the nonlinear susceptibility.

The information about the details of the form of the particle surface¹ is insufficient for direct evaluation of parameters ε , N , N_R , and N_L . We shall choose ε , N , N_R , and N_L in a very similar way and adjust them to the measured quantities. The low precision is only one of the obstacles precluding the accurate estimate of these data. In view of future experimental investigations the following should be accounted for in the adjustment of the particle shape using the parameters N , N_R , and N_L .

(i) The evaluation of N_L , N_R , and N requires the experimental scanning of the surface topography for the individual particle and the tabulating of the surface function $R(\theta, \varphi)$ (23) on the coordinate grid (θ, φ) . Then the Fourier analysis of the surface and the construction of the spectral density S_n^0 versus the number of harmonics n should be made for every particle in the experimental sample.

The characteristic width Δ_n^0 of the spectrum S_n^0 will allow an evaluation of parameters N_L , N_R , and $N = \Delta_n^0 + 1$. An index "0" marks the parameters of the individual particle.

Note that the shape of the particle can be reconstructed without pronounced distortions of spectrum if the surface topography is produced by scanning with the step $\delta \sim a_0$, when a_0 is the lattice constant.

(ii) On the ensemble of realizations of a shape in the experimental sample the parameters N_L , N_R , and N each produce some distribution $P(\nu)$ ($\nu \equiv N_L^0, N_R^0, N^0$). The construction of such a distribution should allow the evaluation of the parameters N_L , N_R , and N [(25') and (26)] (which were introduced for the "typical" particle) as expected values for corresponding distributions $P(\nu)$.

It should be emphasized that the above-mentioned ensemble must be sufficiently numerous for a precise construction of histograms $P(\nu)$. If the different realizations

of shape are independent then for $\nu \sim 10$ about 10^3 spectra S_n^0 should be processed.

D. The size dependence

The final expression for the nonlinear susceptibility that includes the coefficient of the asymmetry has the form

$$\chi_2^i \approx \frac{e^3}{2\hbar^2} \eta \left[\sum_{nmk} \tilde{\chi}_{nmk} \right]^{1/2}, \quad (28)$$

where $\tilde{\chi}_{nmk}$ is a typical term of the sum (14). The transition from sum to the integral in this expression,

$$\sum_n \tilde{\chi}_{nmk} \rightarrow \int \tilde{\chi}_{nmk} \rho(E_n) dE_n, \quad (29)$$

which is possible in the quasiclassical limit, allows us to get the scaling relation

$$\chi_2^i(2\omega) \approx K \eta \left[\frac{a_0}{\bar{R}} \right]^{1/2} \frac{a_{\text{at}}^3}{\mathcal{E}_{\text{at}}} \left[\frac{E_{\text{at}}}{\bar{E}} \right]^{7/4}, \quad (30)$$

where K is a numerical constant and a_{at} , \mathcal{E}_{at} , and E_{at} are the atomic units of the length, electric field, and energy correspondingly; \bar{E} is the characteristic energy of the system.

The estimate (30) is based on a quasiclassical expression for the matrix elements (15) and (16). The scale of the frequency in Eq. (16) is determined by the velocity of the electron in the particle ν . For the metallic particle it can be replaced by the Fermi velocity; thus for the particle with $\bar{R} \approx 5$ nm one gets $\Omega \approx 10^{14}$ s⁻¹. For the semiconductor particle the estimate gives $\Omega \approx 10^{14}$ s⁻¹.

The energy \bar{E} and the numerical coefficient depend on the type of the particle. For the metallic nanocrystals (for example, silver ones) $K \approx 3 \times 10^{-5}$ and

$$\bar{E} \approx [(E_F + 2\hbar\omega)(\hbar\omega)^3]^{2/7} E_F^{-1/7}. \quad (31)$$

For the semiconductor quantum dots (for example, CdSe) $K \approx 2 \times 10^{-4}$; the energy \bar{E} is defined by the width of the energy gap E_g and the energy of the radiation quanta $\hbar\omega$:

$$\bar{E} \approx [E_g(\hbar\omega)^3]^{2/7} (2\hbar\omega - E_g)^{-1/7}. \quad (32)$$

If $2\hbar\omega - E_g \rightarrow 0$ then the energy \bar{E} turns into infinity. In this case our model should be considered as semiquantitative, since the condition of quasiclassically is hardly satisfied.

It can be seen from expression (30) that the nonlinear susceptibility of the individual particle strongly depends on size of particle. Formula (30) may be compared with the experimental data.

IV. RESULTS AND DISCUSSION

A. The size dependence of quadratic susceptibility

In Fig. 3 we have plotted the dependence of the SH enhancement factor G on metallic particle radius. In Fig. 4 the dependence of the enhancement factor G on the semiconductor particle radius is presented. In both cases

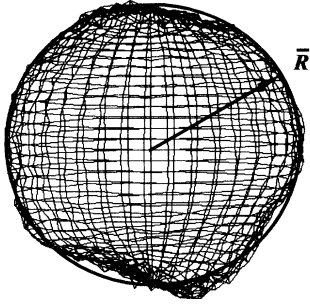


FIG. 5. The surface of the particle [as a function $R(\theta, \varphi)$] computed with the parameters of random modulation: $N_L = 1$, $N_R = 6$; $\varepsilon = 0.2$, $\delta \sim a_0$. In addition, the particle of average radius \bar{R} is shown.

this quantity is proportional to the squared susceptibility of the individual particle $[\chi_2]^2$ (see Sec. II C).

The theoretical formula (30) gives the different types of size dependence due to the different forms of modulation of the particle surface. The modulation by the sufficiently larger number of N of harmonics with $N_{\min} < l < N_{\max}$ seems to be rather probable in the case of both metallic and semiconductor particles. The approximate shape of the particle reconstructed by the computations using (23), (24), and (25) is plotted in Fig. 5. This form of modulation leads to the following type of size dependence for the coefficient of asymmetry:

$$\eta \sim \left[\frac{a_0}{\bar{R}} \right]^2. \quad (33)$$

Then we have from expression (29) the scaling relation

$$[\chi_2']^2 \sim \left[\frac{a_0}{\bar{R}} \right]^5. \quad (34)$$

The corresponding theoretical lines for MN and QD are drawn in Figs. 3 and 4.

B. Comparison with alternative theories

In this paper the role of the particle shape asymmetry is studied with the assumption that the shape distortions are large enough to destroy completely the integrability of the electron motion thus regulating in the ergodic picture. However, it should be stressed that it is not the chaos but the shape asymmetry that gives rise to the effect considered above.

The opposite limiting case of small shape distortions, in which the electron motion remains completely integrable, has been studied in Ref. 6(a). It was shown that small fluctuations of shape can also strongly affect the quadratic optical response of a particle made from a centrosymmetric material (for example, Ag), since a nonzero quadratic susceptibility appears in the dipole approximation because of the shape asymmetry. The assumption of regularity of the electron motion permits the use of perturbation theory based on the coordinate-transformation method analogous to that used in Ref. 21. This approach

yields somewhat weaker size dependence of the G factor for MN, namely, $G \propto |\chi_2|^2 \sim \bar{R}^{-4}$. It appears quite reasonable that the behavior of G does not depend strongly on the degree of regularity of the electron dynamics. However, the application of the perturbation theory to the particles we dealt with in the experiment (with high values of $\bar{R}^{(\text{CdSe})}$ and quasiclassical energy spectrum) seems to be a far-fetched extrapolation that can give only qualitative results.

In comparison with the size dependence given by Eq. (34), the dependence $G(\bar{R})$ obtained in Ref. 6(a) is in much poorer agreement with the experimental data for silver island films. The discrepancy becomes more pronounced when one uses the corrected normalization procedure (see Sec. II C) which takes properly into account the diffuseness of the SH radiation.

Formula (30) has been obtained in the off-resonance assumption, hence, applying our model to the quadratic response of QD, we have ignored the resonant effects which may occur due to the interband optical transitions in sufficiently small particles when the discreteness of electron spectrum becomes pronounced. However, in Ref. 6(b) it was shown that the resonant mechanism can provide the experimentally observed enhancement of the SH generation in CdSe nanocrystallites $G \propto |\chi_2|^2 \sim \bar{R}^{-5}$. This result indicates that a more detailed experimental and theoretical study of interrelation between resonant and nonresonant mechanisms of enhancement in crystallites with $\bar{R}^{(\text{CdSe})} \sim 5$ nm is needed.

The comparison with experiment shows that for each case (MN and QD) the basic tendency in the size dependence is correctly taken into account in the proposed model. However, one should not overestimate the agreement between the theory and experiment because of at least three reasons.

First, some fragments of the experimental data are likely to be not in favor of the proposed theoretical model and may testify to a more complicated (nonmonotonous) character of the real size dependences²² (in Fig. 3 the corresponding clusters of experimental points are indicated with arrows).

Second, the lack of experimental information on the details of the particle shape makes the theory verification incomplete because of a high degree of arbitrariness in the adjustment of the particle shape.

Third, the model we have studied is strongly idealized in many respects. The most important, in our opinion, physical factors which have remained beyond the present consideration are as follows.

(i) The lack of explicit geometrical criteria of complete ergodicity of the motion in three-dimensional billiards: what degree of surface modulation is sufficient to make the electron motion completely ergodic?

(ii) The interaction of electrons. How does it affect the stochasticity of the electron motion? And vice versa, how does the stochasticity modify many-particle excitations, for instance, the surface plasmons which are responsible for resonant enhancement of the local field in MN?

(iii) The electron “spill out” due to the finite height of the boundary potential barrier. Describing the particle

boundary as an infinite potential barrier eliminates this effect, whereas it has been shown²³ that the quadratic optical nonlinearity of a metal system essentially depends on the self-consistent profile of electron density in the selvage region. In this context the question is to what extent our results are sensitive to the form of the boundary potential.

(iv) The finite-temperature effects. How strongly do the kinetics of relaxation in the electron subsystem depend on the particle size?

Each of the aforementioned questions needs its detailed and systematic investigation.

C. Conclusions

These considerations allow us to specify the sense in which one should comprehend the comparison of our theory with the experimental data. First, our interpretation of the experimental results cannot provide an exhaustive explanation of the mechanisms of the size effects because some important physical factors are not taken into account in the model used. Second, applying our theory to the experiment nevertheless shows that those factors which our theory does take into account are able to be responsible for the observed size effects. Third, the

inter-relation of the proposed explanation with alternative ones needs more detailed study within the framework of more realistic models. These statements determine the actual status of the theoretical interpretation given in our paper.

We think that the present work can be an instructive starting point for further experimental and theoretical studies since our results in this field indicate the importance of dynamic stochasticity effects for proper interpretation of nonlinear optical and, as one may expect, other physical phenomena in nanometer-size solid-state structures.

ACKNOWLEDGMENTS

The authors would like to thank L. V. Keldysh, O. Keller, and N. I. Koroteev for valuable discussions, and S. S. Elovikov, N. N. Novikova, and A. I. Ekimov for supplying the samples. The authors acknowledge the support by "Solid State Nanostructures," "Low-dimensional Systems," and "Precision Quantum Electronics" Programs. This work was supported by International Science Foundation Grant No. M12000, by Soros Foundation Grant awarded by the American Physical Society, and INTAS-93 Grant No. 370.

¹For a review, see H. Halperin, *Rev. Mod. Phys.* **58**, 533 (1986); C. Flutzanis, F. Hache, M.-C. Klein, D. Ricard, and P. Roussignol, in *Progress in Optics*, edited by E. Wolf (North-Holland, Amsterdam, 1991).

²A. Nakamura, T. Tokizaki, H. Akiyama, and T. Kataoka, *J. Lumin.* **53**, 105 (1992).

³H. Hosono, J. Abe, J. Lee, T. Tokizaki, and A. Nakamura, *Appl. Phys. Lett.* **61**, 2747 (1992).

⁴S. Ohtsuka, T. Koyama, K. Tsunemoto, H. Nagata, and S. Tanaka, *Appl. Phys. Lett.* **61**, 2953 (1992).

⁵N. M. Lawandy and R. L. MacDonald, *J. Opt. Soc. Am. B* **8**, 1307 (1991).

⁶(a) O. Aktsipetrov *et al.*, *Phys. Lett. A* **117**, 239 (1986); (b) *Pis'ma Zh. Eksp. Teor. Fiz.* **55**, 427 (1992) [*JEPT Lett.* **55**, 435 (1992)].

⁷W. Ekardt, *Phys. Rev. B* **31**, 6360 (1985); F. Hache and D. Ricard, *J. Phys. Condens. Matter* **1**, 8035 (1989); O. Keller *et al.*, in *Proceedings of the 1st NATO Workshop on NFO, Besançon*, edited by D. W. Pohl (Kluwer, Dordrecht, 1993).

⁸B. Eckhardt, *Phys. Rep.* **163**, 205 (1988).

⁹P. V. Elyutin, *Usp. Fiz. Nauk.* **155**, 397 (1988) [*Sov. Phys. Usp.* **31**, 597 (1988)].

¹⁰L. P. Gor'kov and G. M. Eliashberg, *Zh. Eksp. Teor. Fiz.* **48**,

1407 (1965) [*Sov. Phys. JETP* **21**, 940 (1965)].

¹¹V. Buch, R. B. Gerber, and M. A. Ratner, *J. Chem. Phys.* **76**, 5397 (1982).

¹²M. V. Berry and M. Robnik, *J. Phys. A* **17**, 2413 (1984).

¹³M. Feingold and A. Peres, *Phys. Rev. A* **34**, 591 (1986).

¹⁴N. Blombergen, *Phys. Rev.* **174**, 813 (1968).

¹⁵N. I. Koroteev and V. I. Emelyanov, *Usp. Fiz. Nauk* **135**, 345 (1981) [*Sov. Phys. Usp.* **24**, 864 (1981)].

¹⁶A. Ekimov, A. Efros, and A. Onushchenko, *Solid State Commun.* **56**, 921 (1985).

¹⁷N. Blombergen, *Nonlinear Optics* (Benjamin, New York, 1965).

¹⁸L. D. Landau and E. M. Lifshitz, *Statistical Physics, Part 1* (Nauka, Moscow, 1976), Sec. 122.

¹⁹P. V. Elyutin and E. A. Ostrovskaya, *Dokl. Akad. Nauk* **329**, 575 (1993) [*Phys.—Dokl.* **38**, 154 (1993)].

²⁰V. L. Bonch-Bruевич and S. G. Kalashnikov, *The Physics of Semiconductors* (Nauka, Moscow, 1990).

²¹K. F. Ratcliff, in *Multivariate Analysis—V*, edited by P. R. Krishnaiah (North-Holland, Amsterdam, 1980), p. 593.

²²O. Keller, M. Xiao, and S. Bozhevolnyi, *Opt. Commun.* **102**, 238 (1993).

²³A. Liebsch and W. L. Schaich, *Phys. Rev. B* **40**, 5401 (1989).

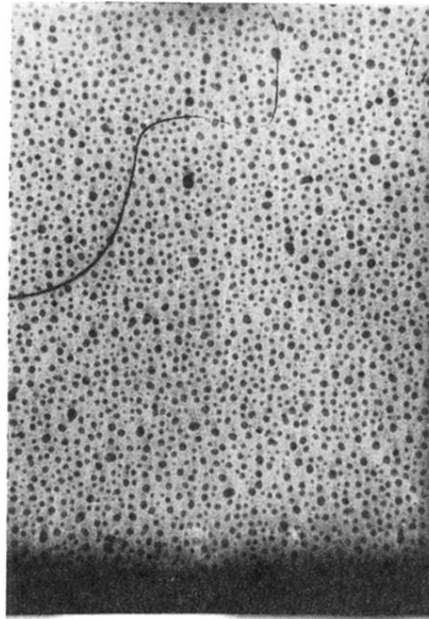


FIG. 1. Typical structure of a silver island film as observed in transmitting electron microscope. The bar is 20 nm long.